S+I− Ionic Formation Mechanism to New Mesoporous Aluminum Phosphonates and Diphosphonates

ARTICLE *in* CHEMISTRY OF MATERIALS · OCTOBER 2004

Impact Factor: 8.35 · DOI: 10.1021/cm048988+

6 AUTHORS, INCLUDING:

Jamal El Haskouri Bennagi
University of Valencia
40 PUBLICATIONS **1,107** CITATIONS

SEE PROFILE

Daniel Beltrán-Porter
University of Valencia
237 PUBLICATIONS **4,437** CITATIONS

SEE PROFILE

Pedro Amorós
University of Valencia
220 PUBLICATIONS **4,986** CITATIONS

SEE PROFILE

S^+I^- Ionic Formation Mechanism to New Mesoporous Aluminum Phosphonates and Diphosphonates

Jamal El Haskouri, Carmen Guillem, Julio Latorre, Aurelio Beltrán, Daniel Beltrán, and Pedro Amorós*

Institut de Ciència dels Materials de la Universitat de Valencia (ICMUV), P.O. Box 2085, 46071-Valencia, Spain

Received June 25, 2004. Revised Manuscript Received August 30, 2004

Pure mesoporous aluminum phosphonates and diphosphonates have been synthesized through an S^+I^- surfactant-assisted cooperative mechanism by means of a one-pot preparative procedure from aqueous solution and starting from aluminum atrane complexes and phosphonic and/or diphosphonic acids. A soft chemical extraction procedure allows opening the pore system of the parent mesostructured materials by exchanging the surfactant without mesostructure collapse. The hybrid nature of the pore wall can be modulated continuously from organic-free mesoporous aluminum phosphates (ALPOs) up to total incorporation of organophosphorus entities (mesoporous phosphonates and diphosphonates). The organic functional groups become basically attached to the pore surface or inserted into the ALPO framework (homogeneously distributed along the surface and inner pore walls) depending on the use of phosphonic or diphosphonic acids, respectively. X-ray powder diffraction, transmission electron microscopy, and surface analysis techniques show that these new hybrid materials present regular unimodal pore systems whose order decreases as the organophosphorus moiety content increases. NMR spectroscopic results not only confirm the incorporation of organophosphorus entities into the framework of these materials but also provide us useful information to elucidate the mechanism through which they are formed.

Introduction

The family of three-dimensional aluminum phosphates known as organic-free mesoporous aluminum phosphates (ALPOs) constitutes, together with zeolites, one of the most important groups of crystalline microporous materials.[1] In fact, since their discovery in 1982,[2] ALPO chemistry stirred great interest mainly due to the attainment of structures showing a broad range of physicochemical properties of potential applications in fields such as catalysis or molecular sieving.[3,4] It is not surprising that ALPO chemistry has evolved similarly to that of zeolites, arousing similar "hot questions" such as those related to the incorporation of heteroelements (usually transition metals to modulate their catalytic properties on the basis of the presence of redox-active sites in the framework) or the expansion of the pore sizes (looking for efficiency in treatments of bulky substrates).[4,5]

In this context, the discovery of the M41S family of mesoporous silicas[6] constituted a breakthrough in the field of zeolite chemistry by offering a way for expanding the available pore sizes to the mesopore range.[7−11] However, pure mesoporous silicas have neutral frameworks, which implies limitations on their applicability in catalysis. Hence, a large variety of mesoporous materials have been prepared using a diversity of procedures conceived to incorporate catalytically active species inside or on the silica walls.[12−15] At first, to extend the chemistry of mesostructured/mesoporous silicas to ALPOs seemed to be a straightforward approach due to their significant electronic and structural similarities. However, this goal proved to be much more difficult than expected owing to problems inherent to the relative chemical complexity of non-silica materials.[16] Over the past few years, and using surfactant-assisted procedures, a diversity of mesostructured/mesoporous ALPOs displaying a variety of topologies (including layered, ordered hexagonal, or disordered wormhole-like materials, which are similar to the MCM-50, MCM-41, and MSU-1 silicas, respectively) have been prepared.[17] Now, in light of the available results, it is possible to outline some tendencies that distinguish

* To whom correspondence should be addressed. Phone: +34-96-3543617. Fax: +34-96-3543633. E-mail: pedro.amoros@uv.es.

(1) Yu, J.; Xu, R. *Acc. Chem. Res.* **2003**, *36*, 481.
(2) Wilson, S. T.; Lok, B. M.; Messina, C. A.; Cannon, T. R.; Flanigan, E. M. *J. Am. Chem. Soc.* **1982**, *104*, 1146.
(3) Davis, M. E.; Saldariaga, C.; Montes, C.; Garces, J.; Crowder, C. *Nature* **1988**, *331*, 698.
(4) Coluccia, S.; Gianotti, E.; Marchese, L. *Mater. Sci. Eng., C* **2001**, *15*, 219.
(5) Hartmann, M.; Kevan, L. *Chem. Rev.* **1999**, *99*, 635.
(6) Kresge, C. T.; Leonowicz, M. E.; Roth, W. J.; Vartuli, J. C.; Beck, J. S. *Nature* **1992**, *359*, 710.
(7) Davis, M. E. *Nature* **2002**, *417*, 813.
(8) Soler-Illia, G. J. A. A.; Sanchez, C.; Lebeau, B.; Patarin, J. *Chem. Rev.* **2002**, *102*, 4093.
(9) Schüth, F. *Angew. Chem., Int. Ed.* **2003**, *42*, 3604.
(10) Polarz, S.; Antonietti, M. *Chem. Commun.* **2002**, 2593.
(11) Stein, A. *Adv. Mater.* **2003**, *15*, 763.
(12) Sayari, A. *Chem. Mater.* **1996**, *8*, 1840.
(13) Corma, A. *Chem. Rev.* **1997**, *97*, 2373.
(14) Ying, J. Y.; Mehnert, C. P.; Wong, M. S. *Angew. Chem., Int. Ed.* **1999**, *38*, 56.
(15) On, D. T.; Desplantier-Giscard, D.; Danumah, C.; Kaliaguine, S. *Appl. Catal., A: Gen.* **2001**, *222*, 299.
(16) Schüth, F. *Chem. Mater.* **2001**, *13*, 3184.

10.1021/cm048988+ CCC: $27.50
Published on Web 10/09/2004

mesostructured/mesoporous ALPOs from the related silicas: (1) in comparison with silicas, layered topologies are more frequently preferred in ALPOs, (2) ALPOs usually present a poorer structural order than the related silicas, and (3) the preparation of mesoporous ALPOs frequently becomes impossible because of the mesostructure collapse during surfactant removal.

With regard to the different types of modified materials currently described, there is abundant information detailing, in the same way as in the case of silicas, the incorporation of a diversity of heteroelements (such as B, Ga, Si, Fe, or Ti) in mesoporous ALPOs.[18−22] The preparation of different mesoporous phosphates (of Zr, Ti, Fe, etc.) is also well documented.[23−29] Notwithstanding, reports on organically modified mesoporous phosphates are very scarce when compared to those dealing with hybrid mesoporous organosilicas.[30] In practice, organic functional groups have been incorporated into mesoporous phosphates by using organosiliceous[31,32] or, principally, organophosphorus reagents.

Organophosphorus reagents have been used as both anionic species able to construct layered or open structures[33,34] (one-pot procedures) and coupling agents for the preparation of hybrid materials based on metal oxides[35] (grafting techniques). Interest in these novel inorganic−organic hybrid composite materials is related to the broad range of potential applications in fields such as catalysis, molecular sieving, and biomedical sciences.[36,37] Although most of the crystalline organophosphonates first prepared were layered, materials containing different metal atoms (such as Al, Cu, Zn, Co, and U) with channel structures have been recently described.[38] Among them, the aluminum phosphonates designated as AlMepO-α and AlMepO-β can be considered as truly microporous organozeolites.[39−41] In contrast, as far as we know, there are only three publications in which mixed mesoporous phosphate/phosphonate (containing Ti[24] or Zr[42]) or mesoporous phosphate/diphosphonate (based on Al[43]) materials are reported. In the case of the Ti and Zr derivatives, by using terminal RPO_3 substituting groups, the phosphonate incorporation into the final materials is limited (<50%) and restricted to the pore surface.[24,42] Dealing with the Al-containing solid, although diphosphonate moieties with bridged methylene groups have been recently used to connect Al centers (in the mesostructured solid),[43] the thermal evolution of the surfactant (to yield a mesoporous material) leads to a significant degradation of diphosphonate groups. As stated by the author, the resulting solid is best described as a mixed phosphate/phosphonate/diphosphonate material (constructed from aluminophosphate-like domains interconnected through bridged organic groups) instead of a pure aluminum diphosphonate.[43]

Following previous work on related materials, we recently discovered a new family of hybrid mesoporous molecular sieves. We have denoted this material series as UVM-9 (for University of Valencia materials-*n*), and some of our preliminary results have been published as a short communication.[44] Now, we report here a more detailed study on the one-pot surfactant-assisted procedure that has allowed us to prepare for the first time mesoporous ALPOs with organically modified surfaces and/or frameworks. This simple and reproducible method facilitates control of the incorporation of organophosphorus moieties, and yields pure mesoporous materials (UVM-9) displaying high chemical homogeneity as well as a good dispersion of the organic groups through a compositional range from organic-free ALPOs to pure mesoporous aluminum phosphonates and diphosphonates. In addition, on the basis of NMR spectroscopic results, we present here a reasonable proposal accounting for the self-assembly mechanism of formation of the UVM-9 materials and simultaneously supplying a wall structural model.

Experimental Section

Synthesis. The method is based on the use of a cationic surfactant ((CTMA)Br = cetyltrimethylammonimum bromide) as a structure-directing agent or supramolecular template (and, consequently, as a porogen after template extraction), and a hydro alcoholic reaction medium (water/2,2′,2″-nitrilotriethanol or triethanolamine, $N(CH_2CH_2OH)_3$, hereinafter TEAH3). The presence of the complexing polyalcohol is key because it has proved its capability of harmonizing the rates of the hydrolytic reactions of the aluminum species in water−phosphoric acid media and the subsequent

(17) Tiemann, M.; Fröba, M. *Chem. Mater.* **2001**, *13*, 3211 and references therein.
(18) Holland, B. T.; Isbester, P. K.; Blanford, C. F.; Munson, E. J.; Stein, A. *J. Am. Chem. Soc.* **1997**, *119*, 6796.
(19) Khimyak, Y. Z.; Klinowski, J. *Phys. Chem. Chem. Phys.* **2000**, *2*, 5275.
(20) Zhao, X. S.; Lu, G. Q.; Whittaker, A. K.; Drennan, J.; Xu, H. *Microporous Mesoporous Mater.* **2002**, *55*, 51.
(21) Gianotti, E.; Oliveira, E. C.; Coluccia, S.; Pastore, H. O.; Marchese, L. *Inorg. Chim. Acta* **2003**, *349*, 259.
(22) Wang, L.; Tian, B.; Fan, J.; Liu, X.; Yang, H.; Yu, C.; Tu, B. *Microporous Mesoporous Mater.* **2004**, *67*, 123.
(23) Antonelli, D. M.; Ying, J. Y. *Angew. Chem., Int. Ed. Engl.* **1996**, *35*, 426.
(24) Bhaumik, A. Inagaki, S. *J. Am. Chem. Soc.* **2001**, *123*, 691.
(25) Jiménez-Jiménez, J.; Maireles-Torres, P.; Olivera-Pastor, P.; Rodríguez-Castellón, E.; Jiménez-López, A.; Jones, D. J.; Rozière, J. *Adv. Mater.* **1998**, *10*, 812.
(26) Kleitz, F.; Thomson, S. J.; Liu, Z.; Terasaki, O.; Schüth, F. *Chem. Mater.* **2002**, *14*, 4134.
(27) Guo, X.; Ding, W.; Wang, X.; Yan, Q. *Chem. Commun.* **2001**, 709.
(28) Serre, C.; Auroux, A.; Gervasini, A.; Hervieu, M.; Férey, G. *Angew. Chem., Int. Ed.* **2002**, *41*, 1594.
(29) Tian, B.; Liu, X.; Tu, B.; Yu, C.; Fan, J.; Wang, L.; Xie, S.; Stucky, G. D.; Zhao, D. *Nat. Mater.* **2003**, *2*, 159.
(30) Sayari, A.; Hamoudi, S. *Chem. Mater.* **2001**, *13*, 3151 and references therein.
(31) Kimura, T. *Chem. Lett.* **2002**, 770.
(32) Kimura, T. *J. Mater. Chem.* **2003**, *13*, 3072.
(33) Cheetham, A. K.; Ferey, G.; Loiseau, T. *Angew. Chem., Int. Ed.* **1999**, *38*, 3268.
(34) Clearfield, A.; Wang, Z. *J. Chem. Soc., Dalton Trans.* **2002**, 2937.
(35) Guerrero, G.; Mutin, P.; Vioux, A. *Chem. Mater.* **2001**, *13*, 4367.
(36) Rocha, G. O.; Rocha, J.; Lin, Z. *Catal. Lett.* **2003**, *89*, 69.
(37) Michel, R.; Lussi, J. W.; Csucs, G.; Reviakine, I.; Danuser, G.; Kettere, B.; Hubbell, J.; Textor, M.; Spencer, N. D. *Langmuir* **2002**, *18*, 3281.
(38) Maeda, K.; Mizukami, F. *Catal. Surv. Jpn*. **1999**, 119.
(39) Maeda, K.; Kiyozumi, Y.; Mizukami, F. *Angew. Chem., Int. Ed. Engl.* **1994**, *33*, 2335.
(40) Maeda, K.; Akimoto, J.; Kiyozumi, Y.; Mizukami, F. *J. Chem. Soc., Chem. Commun.* **1995**, 1033.
(41) Maeda, K.; Akimoto, J.; Kiyozumi, Y.; Mizukami, F. *Angew. Chem., Int. Ed. Engl.* **1995**, *34*, 1199.
(42) Ren, N.; Tang, Y.; Wang, Y. J.; Hu, S. H.; Dong, A. G.; Hua, W. M.; Yue, Y. H.; Shen, J. Y. *Chem. Lett.* **2002**, 1036.
(43) Kimura, T. *Chem. Mater.* **2003**, *15*, 3742.
(44) El Haskouri, J.; Guillem, C.; Beltrán, A.; Latorre, J.; Beltrán, D.; Amorós, P. *Eur. J. Inorg. Chem.* **2004**, 1804.

Table 1. Selected Synthetic and Physical Data for UVM-9 Mesoporous Organophosphonates

sample	phosphonic acid[a]	% solution	% solid[b]	Al:P[c]	d_{100}(XRD)/ nm	a_0[d]/ nm	S_{BET}/ $m^2\,g^{-1}$	BJH pore diam[e]/nm	pore vol/ $cm^3\,g^{-1}$	pore wall thickness[f]/nm
1				1.10(2)	4.86	5.61	633.2	3.23	0.70	2.38
2	M	50	22.3	1.25(2)	4.95	5.72	703.6	2.84	0.75	2.88
3	M	75	45.8	1.15(2)	5.09	5.88	793.9	2.69	0.71	3.19
4	M	100	100	1.24(2)	6.13	7.08	674.9	3.33	0.75	3.75
5	D	50	54.2	0.97(2)	4.96	5.73	655.0	3.41	0.86	2.32
6	D	75	78.1	1.00(2)	5.33	6.15	712.8	3.26	0.85	2.89
7	D	100	100	1.11(2)	6.09	7.03	673.8	3.32	0.63	3.71

[a] M (monophosphonic acid) = $CH_3PO(OH)_2$, and D (diphosphonic acid) = $(OH)_2OP(CH_2)_2PO(OH)_2$. [b] Values estimated from CNH analysis and referred to the P(phosphonate):P(total) molar ratio. [c] Values averaged from EPMA of ca. 50 particles. [d] Cell parameters calculated assuming an MCM-41-like hexagonal cell ($a_0 = 2d_{100}/3^{1/2}$). [e] Pore diameters calculated by using the BJH model on the adsorption branch of the isotherms. [f] Pore wall thickness defined as $a_0 - \phi_{BJH}$.

processes of self-assembly among the resulting inorganic polyanions and the surfactant aggregates.[45] This, in turn, results in a high dispersion of the phosphonate units throughout the pore walls.

Chemicals. All the synthesis reagents are analytically pure, and were used as received from Aldrich [(CTMA)Br, TEAH3, tetraethyl orthosilicate (TEOS), and phosphoric acid] and Fluka [methylphosphonic acid and 1,2-ethylenediphosphonic acid].

Preparative Procedure. A typical one-pot synthesis leading to sample 7 (a pure aluminum diphosphonate; see Table 1) is as follows: (1) Preparation of an adequate aluminum precursor species from a commercial alkoxide. $Al(OBu^s)_3$ (12.7 mL) was slowly added to liquid TEAH3 (26.2 mL) and heated at 150 °C to give aluminum atrane complexes (or alumatranes, compounds containing TEAH3-derived ligands). (2) Addition of the structural-directing (porogen) agent. After cooling of the previous solution to 110 °C, 4.68 g of the (CTMA)Br surfactant was added. (3) Reaction with the phosphonic acid. The solution containing the aluminum source and the template was cooled to 60 °C and mixed with an aqueous solution (120 mL) that contained 7.03 g of 1,2-ethylenediphosphonic acid. After a few seconds, a white suspension appeared. The resulting (mesostructured) powder was filtered off, washed with water and ethanol, and air-dried. (4) Surfactant removal. Finally, the surfactant was chemically extracted from the as-synthesized solid using an acetic acid/ethanol solution (ca. 1 g of powder, 16 mL of acetic acid, and 130 mL of ethanol) by maintaining the suspension of the mesostructured solid in the alcoholic solution, with stirring, for 24 h at room temperature. The final (mesoporous) material was separated by filtration, washed with ethanol, and air-dried. A completely equivalent procedure was followed for obtaining solids with terminal phosphonates (using methylphosphonic acid) or mixed phosphate/phosphonate derivatives (using mixtures of phosphoric and phosphonic acids). In all cases, the molar ratio of the reagents was adjusted to 2Al:3P (H_3PO_4 + phosphonic acid):8TEAH3:0.52(CTMA)Br:270H_2O. Table 1 summarizes the main synthesis variables and physical data concerning the UVM-9 materials prepared in this way.

The versatility and efficiency of this preparative route can be better appreciated as the complexity of the chemical system increases.[46] Thus, this method makes possible the simultaneous incorporation into the UVM-9 walls of other elements different from aluminum (i.e., Si, resulting in organically modified SAPOs). In the same way, it is possible to prepare ALPO-derived mixed phosphonates (i.e., with different organic groups attached to different P atoms). By way of example, we present here the synthesis of an inorganically modified UVM-9 material (denoted as Si-UVM-9, which can be considered as an organically modified SAPO). In this case, the general features of the preparative procedure are as described above. The molar ratio of the reagents was adjusted to 1.93Al:0.7Si:3P (1.5 H_3PO_4 + 1.5 methylphosphonic acid):8TEAH3:0.52(CTMA)Br:270H_2O. The only significant modification consists of the addition of silatranes together with the alumatrane complexes in step 1. In practice, both atrane complexes can be one-pot synthesized by mixing the required amounts of $Al(OBu^s)_3$ and TEOS in TEAH3 (and then heating at 150 °C). The remaining steps were as above.

Physical Measurements. All solids were characterized by elemental CNH analysis and electron probe microanalysis (EPMA) using a Philips SEM-515 instrument (to determine Al, P, and Si). Al/P molar ratio values averaged from EPMA data corresponding to ca. 50 different particles of each sample are summarized in Table 1. X-ray powder diffraction (XRD) data were recorded on a Seifert 3000TT $\theta-\theta$ diffractometer using Cu Kα radiation. Patterns were collected in steps of 0.02° (2θ) over the angular range 1−10° (2θ) for 25 s per step. To detect the presence of some crystalline bulk phase, additional patterns were recorded with a larger scanning step (0.05° (2θ)) over the angular range 10−60° (2θ) for 10 s per step. An electron microscopy study (TEM) was carried out with a JEOL JEM-1010 instrument operating at 100 kV and equipped with a CCD camera. Samples were gently ground in dodecane, and microparticles were deposited on a holey carbon film supported on a Cu grid. Surface area, pore size and volume values were calculated from nitrogen adsorption−desorption isotherms (−196 °C) recorded on a Micromeritics ASAP-2010 automated analyzer. Calcined samples were degassed for 12 h at 110 °C and 10^{-6} Torr prior to analysis. Surface areas were estimated according to the BET model, and pore size dimensions were calculated by using the BJH method. ^{31}P, ^{27}Al, and ^{13}C MAS NMR spectra were recorded on a Varian Unity 300 spectrometer. The MAS probe was tuned at 121.43,

(45) Cabrera, S.; El Haskouri, J.; Mendioroz, S.; Guillem, C.; Latorre, J.; Beltrán, A.; Beltrán, D.; Marcos, M. D.; Amorós, P. *Chem. Commun.* **1999**, 1679.

(46) Cabrera, S.; El Haskouri, J.; Guillem, C.; Latorre, J.; Beltrán, A.; Beltrán, D.; Marcos, M. D.; Amorós, P. *Solid State Sci.* **2000**, *2*, 405.

78.16, and 75.43 MHz for ^{31}P, ^{27}Al, and ^{13}C, respectively, and using a magic angle spinning speed of at least 4.0 kHz. To gain insight into the site geometry and accessibility, as well as the formation mechanism of the UVM-9 materials, we have recorded different series of NMR spectra corresponding to mesoporous dehydrated and rehydrated samples. Mesoporous samples were dehydrated for 24 h at 100 °C under a static air atmosphere. $^{1}H-^{27}Al$ CP-MAS and $^{1}H-^{31}P$ CP-MAS spectra were acquired using ^{1}H $\pi/4$ (5.0 μs) pulses at 299.97 MHz. For ^{31}P NMR MAS and CP-MAS we used an acquisition time of 0.05 s and a relaxation delay of 5.0 s with 300 repetitions. ^{27}Al NMR MAS and CP-MAS spectra were recorded at an acquisition time of 0.05 s and a relaxation delay of 1.0 s with 640 repetitions. ^{13}C NMR CP-MAS spectra were obtained with an acquisition time of 0.05 s and a relaxation delay of 5.0 s with 3000 repetitions. FTIR spectra (KBr pellets) were recorded on a Nicolet spectrophotometer.

Results and Discussion

Synthesis Strategy. The general method reported here to prepare the UVM-9 mesoporous solids involves, together with the participation of a cationic surfactant as template and porogen, an essential procedural feature: the use as reagents of alumatrane complexes (as the source of reactive aluminum species) and commercial phosphonic and/or diphosphonic acids.

Alumatranes can be considered as modified alkoxides which include TEA-like species as ligands (TEA meaning the fully deprotonated triethanolamine ligand).[47] In fact, our synthesis strategy is based on the so-called "atrane route", a simple preparative technique whose details have been reported elsewhere.[46] In practice, such a method (using atrane complexes as inorganic hydrolytic precursors) has allowed us to successfully prepare a diversity of mesoporous single and mixed oxides, as well as aluminum phosphates and silicoaluminophosphates.[45,46,48,49] It must be remarked that alumatrane solutions are easily and quickly prepared without additional crystallization or separation steps. Taking into account the ready formation of relatively inert aluminum atrane complexes, we can say that TEAH3 essentially acts as a "hydrolysis-retarding agent" of the aluminum species, favoring the interaction with phosphate, phosphonate, and/or diphosphonate anions in aqueous solution (under neutral or slightly basic conditions), and the subsequent processes of self-assembly with the $CTMA^{+}$ aggregates.

Moreover, this method also makes possible the incorporation of other elements or organic groups (organosiliceous)[50] without undesired phase segregation phenomena. In practice, the formation of atranes allows harmonizing the hydrolysis and condensation reaction rates of the precursor species of different elements having very different reactivities in water,[46] which favors the preparation through cohydrolysis of complex hybrid organic−inorganic materials displaying high chemical homogeneity.

Incorporation of organic groups into mesoporous silicas has been extensively and successfully studied owing to the potential applications of organosilicas. Thus, a great variety of terminal organic groups ($(RO)_{4-n}SiR'_n$, $1 \le n \le 3$)[30] have been incorporated into the silica matrix through cohydrolysis or posttreatments. In any case, these terminal groups are usually housed in the pore space. As an alternative, a novel strategy based on the use of bridge-bonded silsesquioxanes ($(RO)_3SiR'Si(OR)_3$) led to the incorporation of the organic functional groups embedded in the silica walls (PMO materials).[30,51−53] Thus, working in a mimetic way, we have carried out ALPO surface and framework organic modifications by using RPO_3^{2-} terminal phosphonates (instead of $R'Si(OR)_3$) or $^{2-}O_3PRPO_3^{2-}$-bridged diphosphonates (instead of $(RO)_3SiR'Si(OR)_3$), respectively. Our method also makes possible the progressive incorporation of organic groups which range from organic-free ALPOs (sample 1) to pure mesoporous aluminum phosphonates or diphosphonates (100% organophosphorus groups, samples 4 and 7) to ALPOs with organically modified surfaces (terminal phosphonates, samples 2 and 3) and/or frameworks (bridged diphosphonates, samples 5 and 6). In short, a good selection of reagents, conditions, and procedures allows the full extension of the ALPO derivatives to as broad a family as mesoporous organosilicas.

We mentioned above that, although diphosphonate moieties were used to prepare a mesostructured aluminum methylenediphosphonate,[43] the thermal treatment applied for obtaining the corresponding mesoporous material (by surfactant evolution) leads to a significant decomposition of the methylene groups. According to NMR data, the methylenediphosphonate groups ($\equiv PCH_2P\equiv$) thermally decompose in terminal methylphosphonate ($\equiv PCH_3$) and phosphate groups ($OP\equiv$). Hence, the final solid really is a mixed phosphate/phosphonate/diphosphonate material in which the proportion of the different phosphorus entities seems to be difficult to control.[43] Such a result is not surprising: most of the organic moieties are unstable under the thermal conditions applied for surfactant removal. In fact, in dealing with organosilica materials, chemical extraction has been frequently indicated as the best procedure to remove organic templates without degradation of the hybrid framework.[51−53]A usual requirement to do it involves the use of HCl/ethanol mixtures.[50] This technique, however, is inadequate for aluminum-containing materials: the metal is extracted from the network (in the form of stable chloro complexes) with the subsequent (uncontrolled) compositional changes, and even mesostructure collapse. As expected, treatments based on the use of HCl/ethanol mixtures are too aggressive for the UVM-9 materials and result in mesostructure collapse and redissolution. To avoid this

(47) Verkade, J. G. *Acc. Chem. Res.* **1993**, *26*, 483 and references therein.
(48) El Haskouri, J.; Cabrera, S.; Caldés, M.; Guillem, C.; Latorre, J.; Beltrán, A.; Beltrán, D.; Marcos, M. D.; Amorós, P. *Chem. Mater.* **2002**, *14*, 2637.
(49) Cabrera, S.; El Haskouri, J.; Alamo, J.; Beltrán, A.; Beltrán, D.; Mendioroz, S.; Marcos, M. D.; Amorós, P. *Adv. Mater.* **1999**, *11*, 379.
(50) El Haskouri, J.; Ortiz de Zárate, D.; Guillem, C.; Beltrán, A.; Caldes, M.; Marcos, M. D.; Beltrán, D.; Latorre, J.; Amorós, P. *Chem. Mater.* **2002**, *14*, 4502.
(51) Inagaki, S.; Guan, S.; Fukushima, Y.; Ohsuma, T.; Terasaki, O. *J. Am. Chem. Soc.* **1999**, *121*, 9611.
(52) Melde, B. J.; Holland, B. T.; Blanford, C. F.; Stein, A. *Chem. Mater.* **1999**, *11*, 3302.
(53) Asefa, T.; MacLachlan, M. J.; Coombs, N.; Ozin, G. A. *Nature* **1999**, *402*, 867.

problem, in the case of the UVM-9 solids the elimination of the surfactant from the mesostructured materials has been carried out by an alternative chemical procedure. Thus, we have used acetic acid/ethanol solutions (working at room temperature), which allows cationic $CTMA^+$ surfactant portions to be exchanged with H^+ cations provided by the acetic acid. Moreover, according to EPMA results, this extraction procedure does not alter the Al and phosphonate contents (the corresponding mesostructured and mesoporous solids have identical Al/P molar ratios).

Given that the synthetic course is orchestrated, to a great extent, by the organizing role of the surfactant, our main procedural concern was to establish the optimized conditions to have anionic entities capable of generating the adequate parent mesostructures by assembling with $CTMA^+$ entities. Indeed, the Al:P (H_3PO_4 + phosphonic acid) molar ratio of the reagents was fixed to the final 2:3 value after checking a variety of Al:*x*P (H_3PO_4 + phosphonic acid):4TEAH3:0.26(CTMA)Br:135H_2O starting "compositions", where *x* was varied from 1 to 5. The parameters used to test the "quality" of the resulting solids for each composition were both the mesostructure definition (as indicated by XRD) and the stability after surfactant evolution (monitored by XRD and surface area) of the final mesoporous material. It must be stressed that the experimental apparent pH value (ca. 8 for $x = 1.5$) remains practically unaltered for each *x* value (irrespective of the H_3PO_4/phosphonic acid relative amounts) because of the buffering effect provided by the TEAH3−H_3PO_4−organophosphoric acid system ($pK_2 = 7.2$, $pK = 7.54$, and $pK = 7.8$ for phosphoric acid, methylphosphonic acid, and triethanolamine, respectively).[54,55] Control of pH seems to be critical in avoiding undesired aluminum excesses in the final materials.

Thus, the dominant oxophosphate species under the used reaction conditions in rich aqueous media are HPO_4^{2-}/PO_4^{3-} and RPO_3^{2-} (the concentration of protonated phosphonate is negligible). With regard to the aluminum species, in the absence of phosphorus oxo anions, the tetrahedral $Al(OH)_4^-$ ions are the majority at pH > 5 (resulting from the $Al(H_2O)_6^{3+}$ hydrolysis), and evolve toward hydrated $Al(OH)_3$ at increasing pH.[56] The presence of oxophosphate species must drive the system toward the formation of complex aluminophosphate and/or aluminophosphonate anions involving, very likely, the presence of terminal or aluminum-bridging hydroxyl groups.

Tetrahedral aluminum is ubiquitous (sometimes accompanied by pentacoordination) in solid microporous ALPOs prepared at medium pH values. In fact, it has been noted that the Al_{octa} to Al_{tetra} proportion varies from 1 (variscite) to 0.33 (VPI-5) as the synthesis pH increases from 3 to 6.[57] The Al:P stoichiometry in microporous AlPOs (although they frequently include organic cations) is usually 1, even though lower values have been reported in some cases.[58,59]

In contrast, μ-(hydroxo)aluminum chains (Al_{octa}) are a common structural motif in solid aluminum phosphonates.[39−41] Otherwise, the reported aluminum phosphonates have layered or open-framework structures, and their Al:P stoichiometric ratio is 1 or 0.75.[39−41,60,61] It seems that, as could be expected for crystalline compounds, the Al:P = 1:1 ratio constitutes an "ideal" limit. On the contrary, in the case of some mesoporous AlPOs already known (obtained at high pH values, ca. 8.5−10) significant deviations from the ideal stoichiometry toward defective phosphorus compositions occur (Al:P = 1.55−5.5).[17,18,62−65] In short, these results indicate that noncrystalline networks based on ALPOs are stabilized by condensed aluminum species participating in the pore wall.

In light of the above, our strategy was elaborated for achieving a working Al:P ratio as low as possible, and independent of the ultimate nature of the phosphorus oxo anions. In this way, we try to favor the Al−P−Al moiety alternation in the inorganic walls.

Characterization. We have used EPMA to check the chemical homogeneity of the resulting solids. Summarized in Table 1 are the corresponding Al:P molar ratio values (averaged from data of ca. 50 different particles) of the Si-free samples. EPMA shows that all UVM-9 samples are chemically homogeneous at the micrometer level (spot area ca. 1 μm) with a constant and well-defined composition. In all cases, the UVM-9 solids that contain diphosphonate groups present Al:P proportions close to the Al:P = 1:1 molar ratio, typical of stoichiometric ALPOs, in contrast to the aluminum phosphate/phosphonate materials previously reported (Al:P = 1.37).[43] However, deviations from this 1:1 ratio are detected in the materials that include monophosphonate groups (see Table 1). This fact indicates that the UVM-9 solids may be basically regarded as aluminophosphonates rather than consisting, to a significant degree, of alumina domains connected through organophosphorus moieties. Moreover, the high-angle XRD patterns do not show peaks associated with segregated bulk phases (alumina, aluminum phosphates, or microporous crystalline ALPOs). On the basis of these results, and taking into account the impossibility to condense phosphate, phosphonate, and/or diphosphonate groups among them (originating P−O−P bonds) in aqueous media, it seems reasonable to propose that the UVM-9 materials display a regular distribution of the Al and P atoms along the pore walls. The high chemical homogeneity and dispersion of Al and P atoms indicate that the control of the reactivity that we achieved when using alumatranes as an aluminum source in water−phosphoric acid media[45] is maintained

(54) Popov, K.; Rönkkömäki, H.; Lajunen, L. H. J. *Pure Appl. Chem.* **2001**, *73*, 1641.
(55) Martell, A.; Sillén, L. G. *Stability Constants of Metal-Ion Complexes*; The Chemical Society: London, 1964; p 525.
(56) Baes, C. F.; Mesmer, R. E. *The Hydrolysis of Cations*; Wiley: New York, 1976.
(57) García-Carmona, J.; Rodríguez-Clemente, R.; Gómez-Morales, J. *Adv. Mater.* **1988**, *10*, 46.
(58) *Verified Synthesis of Zeolitic Materials*; *Microporous Mesoporous Mater.* **1998**, *22* (special issue).
(59) Oliver. S.; Kuperman, A.; Lough, A.; Ozin, G. A. *Chem. Mater.* **1996**, *8*, 2391.
(60) Maeda, K.; Hashiguchi, Y.; Kiyozumi, Y.; Mizukami, F. *Bull. Chem. Soc. Jpn.* **1997**, *70*, 345.
(61) Sawers, L.-J.; Carter, V. J.; Armstrong, A. R.; Bruce, P. G.; Wright, P. A.; Gore, B. E. *J. Chem. Soc., Dalton Trans.* **1996**, 3159.
(62) Kimura, T.; Sugahara, Y.; Kuroda, K. *Microporous Mesoporous Mater.* **1998**, *22*, 115.
(63) Luan, Z.; Zhao, D.; He, H.; Klinowski, J.; Kevan, L. *J. Phys. Chem. B* **1998**, *102*, 1250.
(64) Khimyak, Y.; Klinowski, J. *J. Mater. Chem.* **2002**, *12*, 1079.
(65) Tiemann, M.; Fröba, M.; Rapp, G.; Funari, S. S. *Stud. Surf. Sci. Catal.* **2000**, *129*, 559.

when phosphoric acid is partially or totally replaced by phosphonic or diphosphonic acids.

Elemental CNH analysis results reveal that all mesoporous UVM-9 samples are exempt from nitrogen, which confirms the efficiency of the surfactant extraction soft procedure we have used. Moreover, the absence of signals associated with surfactant molecules in their ^{13}C NMR spectra also supports the total elimination of $CTMA^+$. Thus, CNH analysis allows estimating unambiguously the content of organophosphorus groups in the final mesoporous materials (see Table 1). The phosphonate:phosphate stoichiometric ratio in the materials containing diphosphonate species is close to that present in the mother liquor (samples 5 and 7), but it significantly drops (i.e., there is a clear preference for phosphate incorporation) when monophosphonates are involved (samples 2 and 3). Very likely, this difference is related to the capability of the phosphate and diphosphonate groups to act as network building blocks (bridging Al atoms), a role that monophosphate groups do not play (RPO_3 groups are necessarily terminal) in the same extension. Similarly to that occurring in the PMO organosilicas,[51−53] the bridging nature of the diphosphonate entities and their capability to interact through six O atoms facilitate, in practice, their easy incorporation as network-forming groups up to the highest possible level (100% of the total number of P atoms). Hence, the preparation of pure diphosphonate materials becomes possible. Without prejudice to the observed preferential incorporation of phosphate versus monophosphonate groups, the existence of pure aluminum monophosphonates (sample 4) and aluminum diphosphonates (sample 7) is proof of the cooperative ability of the organophosphorus and aluminum moieties to construct stable networks around the surfactant aggregates. In practice, this observation is in good agreement with previous results on organosilicas (with terminal organic groups) suggesting an upper functionalization limit of ca. 40%,[66] depending on the nature of the organic group. Organosilicon species, which only have three coordinating oxygen atoms (with a fourth site occupied by an organic partner), are not able to define a rigid framework around the surfactant aggregates, and require the cooperation of SiO_4^{3-} units (more than 50%) to stabilize the pore wall network. We can see that the intrinsic nature of the UVM-9 materials (with Al:P $\approx$ 1:1) warrants the presence of similar amounts of both types of Al and P network-forming groups. Thus, in the case of aluminum diphosphonates, the net stabilization can be achieved through the cooperative effect of the $^{2-}O_3PRPO_3^{2-}$-bridged diphosphonates and the Al species (leading to practically stoichiometric mesoporous materials). However, all the monophosphonate materials contain a certain "excess" of aluminum (Al:P = 1.15−1.25). As long as the basic characters of the phosphate and phosphonate groups are similar, the origin of this result very likely is related to the monophosphonate incapability to act as an "inner" (bulk) bridging network-forming moiety (as occurs in materials involving terminal organosilicates). To construct the covalent wall network under this restriction requires the structural action of other moieties: silicate units in the case of organosilicate hybrids (until a theoretical limit of 50%) and aluminum bridging species in hybrid AlPOs (it must not be forgotten that condensation of oxophosphorus compounds in the conditions of the synthesis is not possible). Thus, we may consider that the excess of aluminum species in these materials plays a necessary role as a wall stabilizer (i.e., a binder among organophosphorus moieties), and this role becomes possible just because of the ability of aluminum to adopt both tetrahedral and octahedral environments. The coordination index of the aluminum atoms can increase from IV to VI by interaction with water molecules or through the formation of Al−OH bonds. Now, it must be noted that, according to the stoichiometric restrictions and the nature of the synthesis, the necessary electroneutrality of the materials requires a certain negative net charge on the hybrid pore walls for matching with the surfactant cationic portions. In practice, the presence of a certain amount of hydroxyl groups in the mesoporous UVM-9 materials is required for charge balancing (we will return to this point later on).

Shown in Figures 1 and 2, which correspond to mesostructured (Figures 1i and 2i) and mesoporous (Figures 1ii and 2ii) UVM-9 materials, is the evolution of the low-angle XRD patterns with the phosphonate or diphosphonate content in the solids. All solids display XRD patterns with at least one strong diffraction peak, which is typical of mesostructured/mesoporous materials prepared through surfactant-assisted procedures. This peak is usually associated with the (100) reflection

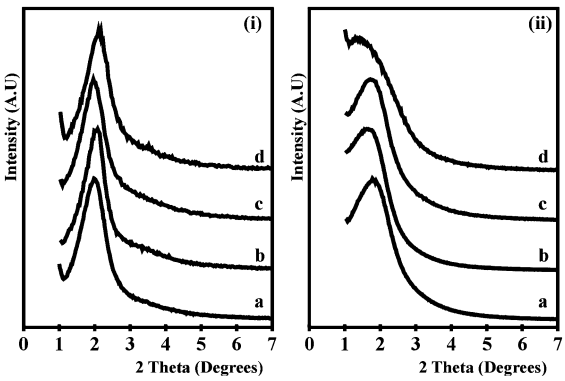

Figure 1. Low-angle XRD patterns of (i) mesostructured and (ii) mesoporous UVM-9 materials (pure ALPO and aluminum phosphate/monophosphonate): (a) sample 1; (b) sample 2; (c) sample 3, (d) sample 4.

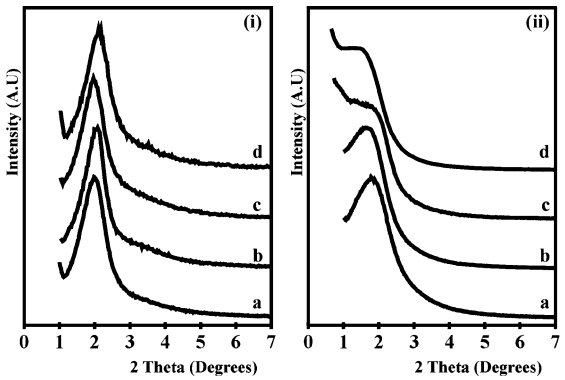

Figure 2. Low-angle XRD patterns of (i) mesostructured and (ii) mesoporous UVM-9 materials (pure ALPO and aluminum phosphate/diphosphonate): (a) sample 1; (b) sample 5; (c) sample 6, (d) sample 7.

(66) Burkett, S. L.; Sims, S. D.; Mann, S. *Chem. Commun.* **1996**, 1367.

when an MCM-41-like lattice is assumed. In the case of the mesostructured solids (Figures 1i and 2i), apart from this intense (100) reflection, we can observe one broad signal (a shoulder of the (100) peak) of very low intensity, which can be associated with the overlapped (110) and (200) reflections. This feature can be associated with the existence of small domains with a partially ordered hexagonal (H_o) mesopore array. Otherwise, the evolution of the (100) fwhm indicates an increasing disorder as the phosphonate content increases. On the other hand, there is a clear loss of order in the case of the mesoporous solids (Figures 1ii and 2ii). Indeed, their XRD patterns only display a broad signal, which is characteristic of disordered hexagonal (H_d) or wormhole-like pore systems. When comparing the mesoporous materials with their corresponding mesostructured parents, we can observe that the surfactant evolution results in a significant broadening of the intense (100) peak together with a shift in its position toward lower 2θ values, which agrees with results in previous publications on related mesoporous ALPOs.[62−64] It can then be concluded that surfactant removal implies a significant loss of order in the pore system (with regard to the parent mesostructured materials), despite the soft chemical extraction procedure we have used. Also, the d_{100} reticular distance (and consequently the a_0 cell parameter) increases with the phosphonate or diphosphonate content, occurring for both the mesostructured and mesoporous series (see Table 1). This is a not surprising result. In fact, as phosphate/phosphonate substitution progresses, one obtains a larger molecular volume and a smaller net connectivity, both factors favoring a lower density of the substituted material. The experimentally observed smooth variation of the broadness and the position of the peak, in both series of materials, allows a certain character of "solid solutions" to be recognized in them. All the evidence indicates that we are dealing with materials having a reasonably good statistical distribution of phosphate and organophosphorus moieties in the walls.

Most of the UVM-9 samples are unstable under an electron beam, and evolve to more disordered materials. This effect is more pronounced as the organic content increases. Obviously, this fact hinders the TEM detailed study approach. Notwithstanding, the information from TEM images, acquired in short times, fully correlates with XRD observations (Figure 3). The observation in all cases of a dominant (single-type) particle morphology (with highly disordered hexagonal or wormhole-like pore system arrays) supports the monophasic nature of the UVM-9 solids, and allows discarding phase-segregation processes. Although, in general, the main motive of the mesopore organization is defined by disordered hexagonal or wormhole-like arrays, there are some cases in which we have detected the presence of isolated and small ordered hexagonal domains (especially dealing with mesostructured materials and/or samples having a relatively low proportion of organophosphorus entities). Very likely, these ordered domains should account for the weak and unresolved peaks detected, together with the (100) reflection, in some XRD patterns.

Mesoporosity of the UVM-9 materials is further illustrated by the N_2 adsorption−desorption isotherms (Figures 4 and 5). In all cases, the curves show one well-defined step at intermediate partial pressures ($0.3 < P/P_0 < 0.8$) characteristic of type IV isotherms with an H1 small hysteresis loop (as defined by IUPAC). This adsorption should be due to the capillary condensation of N_2 inside the mesopores, and is related to a pore diameter in the mesopore range. Moreover, the sharpness of this step indicates the uniformity of the mesopores. On the other hand, while the progressive incorporation of diphosphonate groups practically does not affect the pore size (estimated by using the adsorption branch of the isotherms and applying the BJH model) of the final materials (ca. 3.3 nm), a slightly higher dispersion in pore sizes is observed in the case of the aluminum monophosphonates (2.7−3.3 nm). Although XRD and TEM data suggest a progressive loss of order as the organophosphorus content increases, the relative sharpness of the adsorption steps and the high BET surface area and pore volume values indicate a reasonable uniformity of the mesopores, which can be considered unusual in non-silica-based materials. The experimental surface area and pore volume values (per gram) are similar for all the UVM-9 materials. Such an

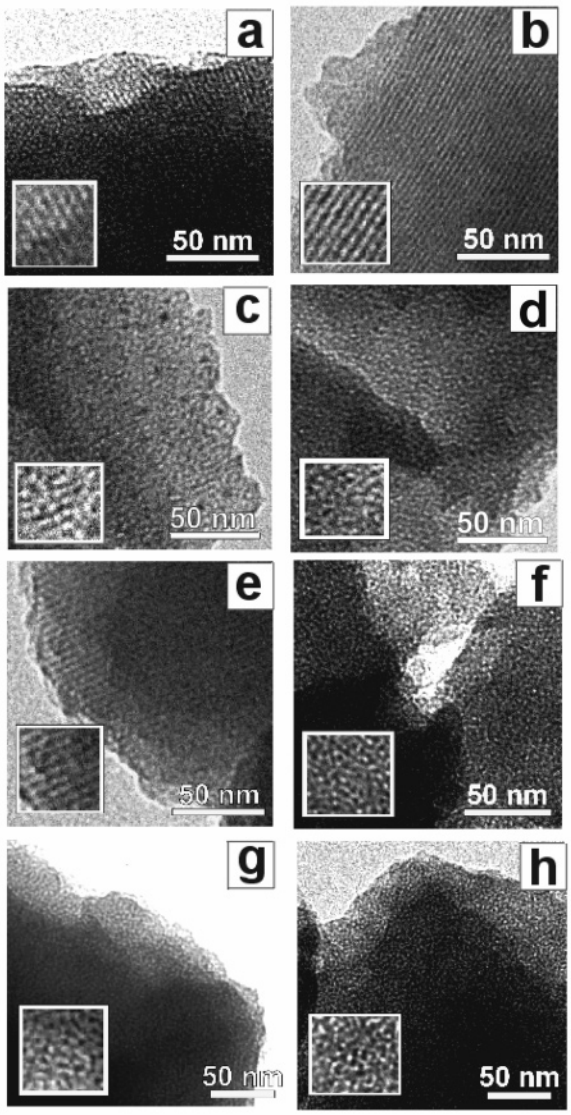

Figure 3. Selected TEM micrographs: (a) sample 1; (b, c) sample 2; (d, e) sample 5; (f) sample 3; (g) sample 4; (h) sample 7. The insets show enlarged (2×) images.

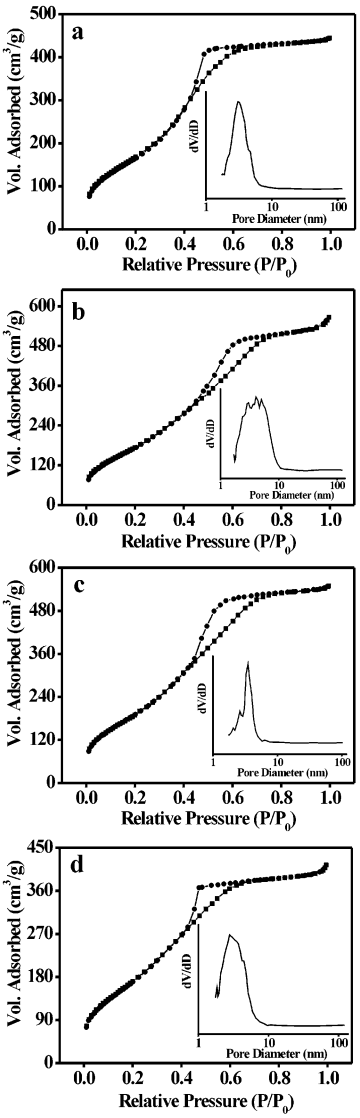

Figure 4. N_2 adsorption−desorption isotherms for ALPO and aluminum phosphate/monophosphonate derivatives: (a) sample 1; (b) sample 2; (c) sample 3; (d) sample 4. The insets show the BJH pore size distributions from the adsorption branch of the isotherms.

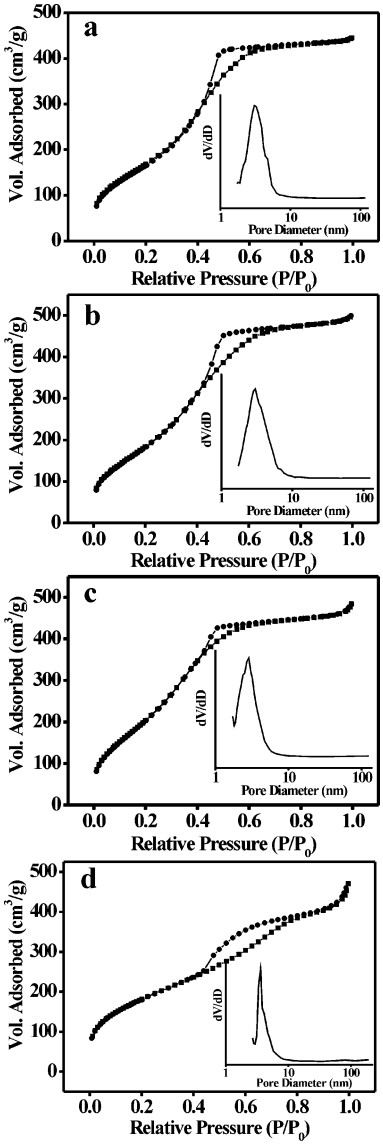

Figure 5. N_2 adsorption−desorption isotherms for ALPO and aluminum phosphate/diphosphonate derivatives: (a) sample 1; (b) sample 5; (c) sample 6; (d) sample 7. The insets show the BJH pore size distributions from the adsorption branch of the isotherms.

observation could be related to the gradual decrease of the density of the sample with increasing amount of phosphonate or diphosphonate units replacing phosphate groups. In fact, the thickness of the pore walls ($W_t = a_0 - \phi_{BJH}$) increases with the organic functionalization, which should be in agreement with the incorporation of organophosphorus moieties in the walls. Both the incorporation of organic groups embedded in the pore walls and the increasing proportion of (octahedral) Al atoms would work cooperatively to form thicker (although softer, according to TEM observations) walls. In the case of aluminum monophosphonates, the relatively higher proportion of Al atoms (Al:P = 1.15−1.25) would favor the growth of larger pore walls.

EPMA results corresponding to Si-UVM-9 show a high chemical homogeneity, with a good dispersion of Al, P, and Si atoms (Al:P = 1.23, Al:Si = 25). Moreover, CNH analysis shows that 20% of the P atoms correspond to methylphosphonate groups. Its low-angle XRD pattern (Figure 6a) displays only the intense and broad (100) peak (d_{100} = 4.82 nm), indicating a disordered hexagonal pore organization. As expected, this pattern is very similar to those observed for the UVM-9 materials. The N_2 adsorption−desorption isotherm (Figure 6b) also presents a well-defined adsorption step, which is characteristic of mesoporous materials (S_{BET} = 509.5 m^2/g; pore size(BJH) 2.90 nm; pore volume 0.45 cm^3/g).

^{13}C and ^{31}P MAS NMR spectra confirm the incorporation of phosphonate and/or diphosphonate groups in the final mesoporous UVM-9 solids. Moreover, NMR data provide useful information on their evolution as the functionalization level increases. Thus, the ^{13}C MAS NMR spectra of the final materials (Figure 7) exhibit either one doublet centered at 18.2 ppm with $J(^{31}P)$ = 10 (phosphonate derivatives) or one single peak at 21.5 ppm (diphosphonate derivatives), which are unambiguously attributable to methyl and ethylene groups covalently linked to phosphorus atoms, respectively. Also, there is no signal attributable to traces of $CTMA^+$ and/or TEAH3 in the spectra. This result corroborates the

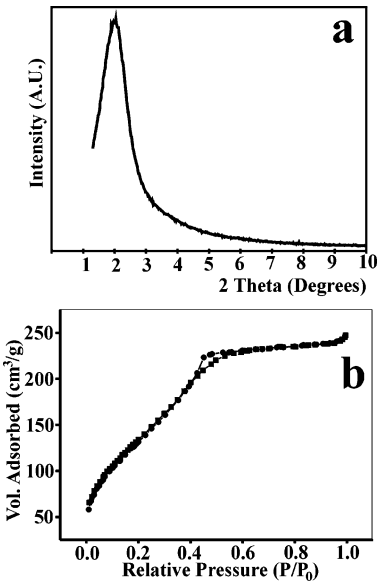

Figure 6. XRD pattern (a) and N_2 adsorption−desorption isotherm (b) for Si−UVM-9.

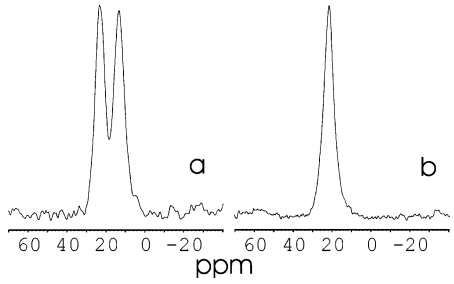

Figure 7. ^{13}C MAS NMR spectra (recorded under ambient conditions) of selected mesoporous materials: (a) sample 4; (b) sample 7.

Table 2. NMR Data of Anhydrous Mesoporous UVM-9 Materials

	^{31}P NMR		^{27}Al NMR			
sample	δ/ppm (phosphate)	δ/ppm (phosphonate)	δ/ppm (T_d)	% T_d	δ/ppm (O_h)	% O_h
1	−24.5		44.8	53	−8.9	47
2	−21.5	17.5	43.7	50	−8.0	50
3	−21.5	16.4	45.3	40	−5.5	60
4		12.4	48.0	26	−9.1	75
5	−23.2	15.9	43.5	51	−8.0	49
6	−24.7	14.5	44.2	47	−8.9	53
7		11.6	46.7	32	−6.9	68

efficiency of the surfactant exchange procedure, which agrees with the elemental CNH analysis data.

On the other hand, it must be remarked that the ^{31}P and ^{27}Al NMR spectra of all the mesoporous solids reported here are very sensitive to humidity, indicating significant interactions between water molecules and hydrophilic portions of each sample. Obviously, the noticed spectral variations must reflect structural features of the materials. Therefore, we have recorded the effect of the water uptake on the NMR spectra of some selected compounds, ranging from dry (anhydrous) to wet (water-vapor-saturated air at room temperature) conditions. Tables 2 and 3 gather the results corresponding to a set of UVM-9 materials, including the pure homoanionic (anhydrous and wet) compounds (aluminum phosphate or ALPO, sample 1; aluminum methylphosphonate, sample 4; aluminum ethylenediphosphonate, sample 7) and several heteroanionic (phosphate/phosphonate) anhydrous materials (samples 2, 3, 5, and 6).

Table 3. Selected NMR Data of Hydrated Mesoporous UVM-9 Materials

	^{31}P NMR	^{27}Al NMR			
sample	δ/ppm	δ/ppm (T_d)	% T_d	δ/ppm (O_h)	% O_h
1	−17.5	51.2	25	−6.4	75
4	14.4	50.3	10	−7.0	90
7	14.1	53.1	15	−5.8	85

The ^{31}P NMR spectra of the anhydrous homoanionic mesoporous materials (samples 1, 4, and 7) display only one single and broad (fwhm ca. 12 ppm) signal (centered at −24.5, 12.4, and 11.6 ppm, respectively; see Figures 8 and 9 and Table 2). The spectra of the heteroanionic materials show two peaks whose intensities are weighted

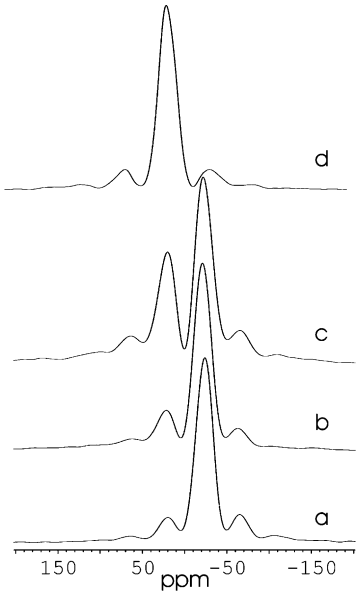

Figure 8. ^{31}P MAS NMR spectra of dehydrated samples (ALPO and aluminum phosphate/monophosphonate derivatives): (a) sample 1; (b) sample 2; (c) sample 3; (d) sample 4.

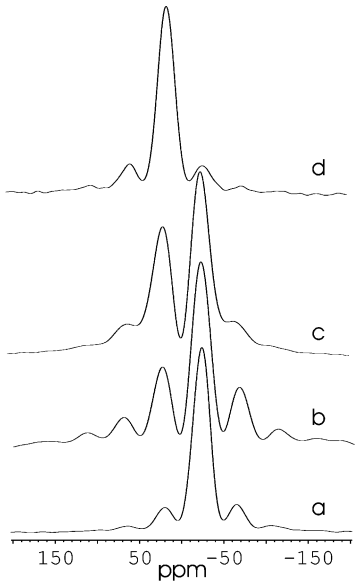

Figure 9. ^{31}P MAS NMR spectra of dehydrated samples (ALPO and aluminum phosphate/diphosphonate derivatives): (a) sample 1; (b) sample 5; (c) sample 6; (d) sample 7.

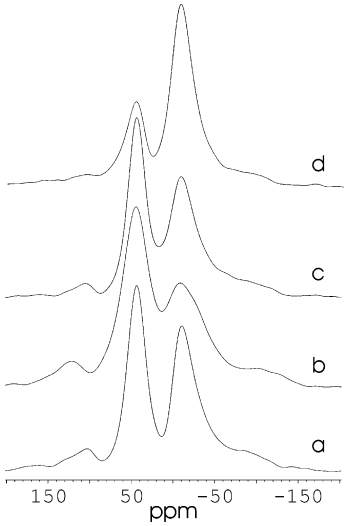

Figure 10. ^{27}Al MAS NMR spectra of dehydrated UVM-9 materials (ALPO and aluminum phosphate/monophosphonate derivatives): (a) sample 1; (b) sample 2; (c) sample 3; (d) sample 4.

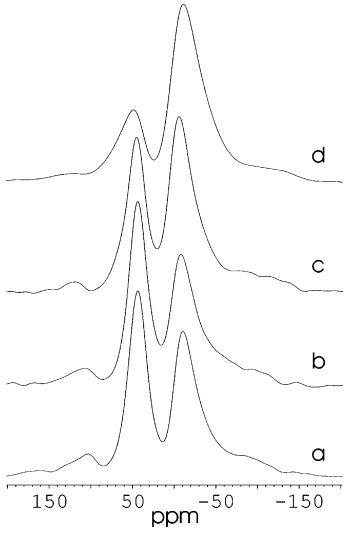

Figure 11. ^{27}Al MAS NMR spectra of dehydrated UVM-9 materials (ALPO and aluminum phosphate/diphosphonate derivatives): (a) sample 1; (b) sample 5; (c) sample 6; (d) sample 7.

according to their phosphate:phosphonate ratios (in good accordance with the CNH analysis data). Indeed, as the phosphonic:phosphoric acid ratio decreases (from sample 4 to sample 2, and from sample 7 to sample 5), we can observe an increase in the intensity of the signal associated with phosphate groups (−24 ppm) and a concomitant decrease in that associated with phosphonate groups (around 12 ppm). A first glance the $\delta(^{31}P)$ values in Table 2 show that the phosphate signal appearing near −24 ppm is relatively insensitive to the composition (phosphate-to-phosphonate ratio), whereas a downfield shift of around 4 ppm (with regard to its position in the spectra of the homoanionic compounds) is observed for the ^{31}P signal associated with phosphonate groups. If we take into account the broadness (±6 ppm) of the ^{31}P NMR signal in the spectra of these amorphous materials, we can realize that the peaks are centered at the mean values previously reported for crystalline compounds of similar compositions. Thus, we can reasonably conclude that the observed ^{31}P NMR spectra are typical of tetrahedral phosphate or organophosphorus groups connected to aluminum centers, which define an essentially P−O−Al alternating covalent network based on acid−base interactions between aluminum-based cations and phosphate/phosphonate anions.

Shown in Figures 10 and 11 are the ^{27}Al MAS NMR spectra of the anhydrous mesoporous UVM-9 materials. All solids have spectra including two resonance signals at δ ca. −9 and 45 ppm. These signals are indicative of hexa- and tetracoordinated Al centers, respectively.[62−64] By deconvoluting the spectra, it becomes possible to estimate the relative proportions of both kinds of aluminum species (see Table 2). In the case of ALPO (sample 1), the tetrahedral Al sites are the majority (ca. 53%). The proportion of octahedral Al sites increases as more of the phosphonate (ca. 50% for sample 2 and 60% for sample 3) or diphosphonate (ca. 50% for sample 5 and 53% for sample 6) groups are incorporated, and finally they become dominant in samples 4 (ca. 75%) and 7 (ca. 68%). Very likely, this evolution reflects that the necessary charge balance is achieved by incorporating hydroxyl groups into the aluminum coordination sphere. The absence of significant shifts of the ^{27}Al signals of both tetrahedral and octahedral aluminum sites indicates that, irrespective of the phosphonate/phosphate content, the aluminum building blocks involved in the mesoporous anhydrous UVM-9 materials are similar.

Most of the reports on microporous ALPOs including data about ^{31}P NMR signals give chemical shift values in the −19 to −31 ppm range, which are referred to tetrahedral phosphorus covalently bonded (via oxygen atoms) to aluminum centers with, preferably, tetrahedral coordination.[67] These downfield shifts of the ^{31}P NMR signal seem associated with oxygen protonation or with an increase of the Al_{octa}:Al_{tetra} ratio in the first coordination sphere of phosphorus atoms in AlPOs.[64] Otherwise, crystalline phosphonates[66] with an Al_{octa}:Al_{tetra} ratio of 0.5 originate ^{31}P NMR signals in the 0−15 ppm range (depending on the Al−O−P bond angle), but no data are known for compounds having other Al_{octa}:Al_{tetra} ratios. As stated above, in the case of the anhydrous mesoporous UVM-9 materials, the $\delta(^{31}P)$ associated with phosphate groups remains practically unaffected, whereas the phosphonate signal shows a gradual downfield shift as the phosphonate content increases (Table 2). It must be noted that, in both UVM-9 series (homoanionic and heteroanionic), the Al_{octa}:Al_{tetra} ratio increases with the phosphonate content, which would account for the observed phosphonate signal evolution. Actually, the same effect could be expected to operate on the signal associated with phosphate groups, but the shift, if any, is very small. A possible explanation for such a behavior would be related to a certain preference of phosphate and phosphonate groups for tetrahedral or octahedral Al sites, respectively, which would result, in turn, in a certain wall heterogeneity.

In short, in contrast to those of previously reported materials,[43] the NMR spectral data of the anhydrous

(67) Rocha, J.; Kolodziejski, W.; He, H.; Klinowski, J. *J. Am. Chem. Soc.* **1992**, *114*, 4884.

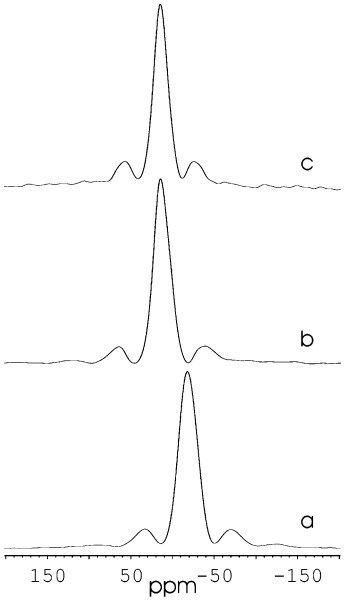

Figure 12. ^{31}P MAS NMR spectra of selected hydrated samples: (a) sample 1; (b) sample 4; (c) sample 7.

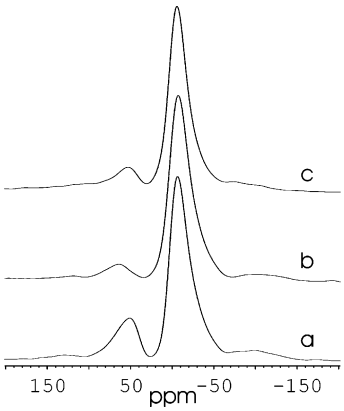

Figure 13. ^{27}Al MAS NMR spectra of selected hydrated samples: (a) sample 1; (b) sample 4; (c) sample 7.

mesoporous UVM-9 materials, considered as a whole, indicate that these solids can be regarded as truly aluminum phosphonate/diphosphonate/phosphate materials and pure aluminum phosphonate/diphosphonate derivatives with a reasonably good alternation of P and Al centers.

We have mentioned that the ^{31}P and ^{27}Al NMR spectra of the UVM-9 samples are very sensitive to humidity. To study this effect, a set of anhydrous UVM-9 samples has been hydrated under a controlled water-saturated air atmosphere at room temperature. Shown in Figures 12 and 13 are the ^{31}P and ^{27}Al NMR spectra of the resulting wet UVM-9 materials (samples 1, 4, and 7). It must be remarked that the spectral changes are completely reversible for each one of these materials after alternating dehydration−rehydration cycles. While the spectra of the wet materials maintain the general features appearing in those corresponding to the anhydrous samples, we can observe that hydration results in a systematic downfield shift for all the ^{31}P signals. This shift is relatively pronounced for the signal associated with phosphate groups ($\Delta\delta \approx 6$ ppm) and significantly smaller for that of organophosphorus groups ($\Delta\delta \approx 2$ ppm) (see the data in Table 3). The observed effect is presumably due to the interaction of water molecules with acid POH groups, and it has been previously noted for other mesoporous ALPOs.[63,64] Taking into account the magnitude of the shift relative to the fwmh of the signal, it seems evident that the number of protonated phosphate groups in sample 1 is significantly higher than the number of protonated phosphonate groups in sample 4 or 7. In general, the effective incorporation into the network of organophosphorus moieties in mesoporous and microporous ALPOs (and related materials) implies connectivity with Al centers through all available oxygen atoms (3O). This requisite is more restrictive in the case of terminal phosphonates. Hence, taking into account the nature of organophosphorus moieties, and on the basis of the NMR data, we can practically discard the presence of protonated phosphonates or diphosphonates in samples 4 and 7.

In the case of the ^{27}Al NMR spectra, hydration of the UVM-9 materials gives rise to significant spectral changes affecting not only the peak positions but also the relative intensity of the signals associated with hexa- and tetracoordinated Al centers. It is evident that the amount of octahedral aluminum centers always increases with hydration. Indeed, in the case of ALPO (sample 1), more than half (ca. 53%) of the Al centers are tetrahedral in the anhydrous solid, while the octahedral Al centers become dominant (ca. 75%) after hydration. This suggests that there are a certain proportion (ca. 28%) of tetrahedral aluminum atoms (at the wall surface) which are able to expand their coordination sphere by accepting two water molecules. In this way, they should become octahedral centers, while keeping their original position. In the cases of aluminum phosphonate and aluminum diphosphonate (samples 4 and 7), the changes in the Al coordination after hydration are less pronounced (ca. 15% and 17% for samples 4 and 7, respectively), which is clearly related to the high proportion of octahedral Al sites (associated with the presence of OH groups bonded to Al atoms) in the anhydrous materials (ca. 75% and 68% for samples 4 and 7, respectively). On the other hand, whereas hydration results in a small downfield shift (ca. 2 ppm) of the peak associated with octahedral aluminum, the effect on the signal of tetrahedral aluminum, although similar, is remarkably higher (ca. 5 ppm). At this point, it should be remembered that these materials were prepared from aqueous solution (in wet form), and consequently, the dehydrated (anhydrous) samples should include a significant part of the highly distorted tetracoordinated Al centers (generated by the loss of two coordinated water molecules from hexacoordinated Al centers). The apparent shift after hydration could be due, to a great extent, to the disappearance of the contribution to the signal associated with the presence of highly distorted tetracoordinated Al centers. In any case, it must be stressed that the dehydration−rehydration processes are reversible, and both the Al_{octa}:Al_{tetra} values and the chemical shifts of the ^{27}Al and ^{31}P NMR signals are recovered after successive dehydration−rehydration cycles.

Formation Mechanism. In the absence of ion-mediated species at the surfactant−aluminum phosphate/phosphonate interface, the parent-mesostructured UVM-9 materials constitute an example of surfactant-templated

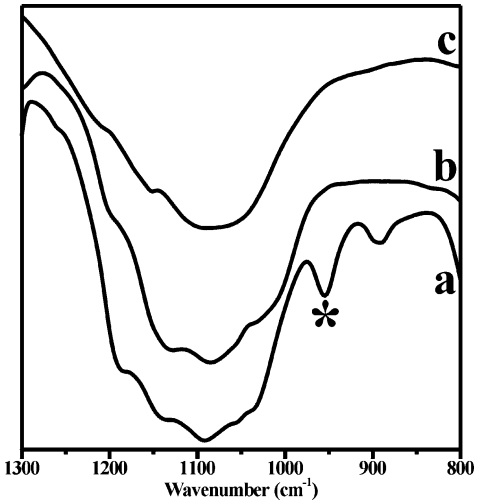

Figure 14. IR spectra of (a) sample 1, (b) sample 7, and (c) sample 4.

materials formed through an S^+I^- ionic mechanism.[69] The charge matching at the interface must occur between cationic surfactant aggregates and anionic aluminum phosphate and/or aluminum phosphate/diphosphonate moieties. Thus, the aluminum phosphate/organophosphonate walls must retain a certain negative net charge in the parent-mesostructured UVM-9 materials.

On the basis of the NMR data, it seems reasonable to propose that the aluminum phosphate/organophosphonate walls are able to compensate the positive surfactant charge through two different mechanisms. On one hand, the presence of $\equiv P-O^-$ units (from phosphate groups connected to aluminum atoms) would allow neutralizing the charge of one $CTMA^+$ cation per $\equiv P-O^-$ group. On the other hand, the ability of the aluminum species to increase their coordination number from IV to VI (by interaction with water molecules and/or hydroxyl groups) would make possible neutralization of the charge of $CTMA^+$ cations on account of the presence of $Al-O^-$ groups at the wall surface.

In any case, the structural connectivity seems to require organophosphorus entities sharing, at least, three oxygen atoms, which would be difficult in the framework of RPO_2OH moieties.[70] Let us see. In the case of the anhydrous mesoporous aluminum diphosphonate (sample 7), the NMR results (small downfield $\Delta\delta(^{31}P) \approx 2$ ppm after hydration) allow us to practically discard a charge compensation mechanism implying protonation of $^{2-}O_3PRPO_3^{2-}$ groups. This hypothesis is additionally supported by the absence of any band associated with a stretching P−(OH) mode (υ(P−(OH) = 850−950 cm^{-1})[71,72] in the FTIR spectrum (Figure 14). We can conclude, therefore, that all the oxygen atoms from organophosphorus moieties are involved in Al−O bonds, this connectivity warranting the wall cohesion. If so, during the formation of the corresponding meso-

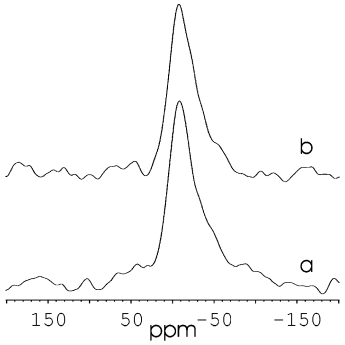

Figure 15. $^1H-^{27}Al$ CP-MAS NMR spectra of sample 7 (a) and sample 4 (b).

structured parent, the charge matching with the $CTMA^+$ surfactant portions basically must rely on the Al sublattice, and more specifically on octahedral aluminum sites close to the wall surface. In fact, the ^{27}Al NMR spectrum of sample 7 is consistent with the presence of a high proportion of octahedral Al centers (ca. 68%) maintaining an Al:P ratio close to 1. Moreover, the $^1H-^{27}Al$ CP-MAS spectrum of sample 7 (Figure 15a) shows an enhancement of the intensity of the line from the hexacoordinated Al centers relative to that associated with tetracoordinated ones (practically at the background level), which indicates the closeness of Al to OH groups. It must be stated that EPMA and CNH analysis of the parent-mesostructured sample 7 resulted in an Al:$CTMA^+$ molar ratio of 1.59, which means that the molar ratio of permanent octahedral Al sites vs $CTMA^+$ ions is close to 1 (1.1). These octahedral Al sites must be associated with the presence of OH groups linked to Al atoms. In conclusion, in the case of the aluminum diphosphonates, it can be stated that a negative net charge equivalent to the existence of ca. 68% $Al-O^-$ groups (with respect to the total Al sites) is required to achieve a good matching with the surfactant aggregates.

In the case of the aluminum phosphonate (sample 4), it should be possible to reproduce a similar reasoning about the anion connectivity from the NMR data. Thus, as in the case of the aluminum diphosphonate, it can be thought that the formation of $Al-O^-$ groups is the only charge-compensating working mechanism. Moreover, the $^1H-^{27}Al$ CP-MAS spectrum of the anhydrous sample (Figure 15b) shows only a single signal at ca. 50 ppm, which is clearly attributable to octahedral Al−OH moieties. Concerning the parent-mesostructured sample 4, EPMA and CNH analyses, as well as NMR data, lead to calculated values of the Al:$CTMA^+$ and Al_{octa}(anhydrous sample):$CTMA^+$ molar ratios of 1.75 and 1.3, respectively. Taking into account that the XRD patterns of the mesostructured and mesoporous samples 4 and **7** display the intense (100) peak at very close 2θ values (and considering the similar pore size dimensions), it seems reasonable to assume that the surfactant aggregates have a similar charge density at the micelle surface for both mesostructured materials. Under this assumption, the above values suggest that the "excess" (7%) of Al atoms in sample 4 (Al/P = 1.24) corresponds to permanent octahedral aluminum sites not required for the matching mechanism, and they should be presumably located inside the pore walls (nonaccessible to water molecules).

(68) Maeda, K.; Kiyozumi, Y.; Mizukami, F. *J. Phys. Chem. B* **1997**, *101*, 4402.
(69) Huo, Q.; Margolese, D. I.; Ciesla, U.; Feng, P.; Gier, T. E.; Sieger, P.; Leon, R.; Petroff, P. M.; Schüth, F.; Stucky, G. D. *Nature* **1994**, *368*, 317.
(70) Mutin, P. H.; Guerrero, G.; Vioux, A. *C. R. Chim.* **2003**, *6*, 1153.
(71) Corbridge, D. E. C.; Lowe, E. J. *J. Chem. Soc.* **1954**, 493.
(72) Barja, B. C.; Herszage, J.; Alfonso, M. *Polyhedron* **2001**, *20*, 1821.

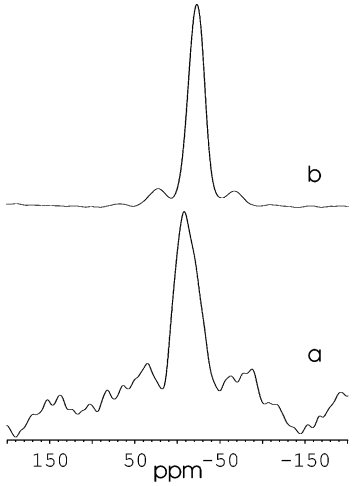

Figure 16. $^{1}H-^{27}Al$ CP-MAS NMR spectra (a) and $^{1}H-^{31}P$ CP-MAS NMR spectra (b) of sample 1.

Finally, in the case of the aluminum phosphate or ALPO (sample 1), the $^{1}H-^{27}Al$ and $^{1}H-^{31}P$ CP-MAS NMR spectra prove that both phosphate and aluminum species participate in the matching mechanism. Thus, single signals assignable to octahedral AlOH and POH entities are clearly observed (Figure 16). Moreover, the FTIR spectrum shows (as in all samples containing phosphate) a well-resolved band at ca. 950 cm^{-1} (indicated in Figure 14) associated with the stretching P−(OH) vibrations.[71,72] The analyses of the corresponding parent-mesostructured compound give Al:$CTMA^{+}$ and Al_{octa}(anhydrous sample):$CTMA^{+}$ molar ratios of 1.56 and 0.78, respectively, and then 22% of the negative charge, at least, must be provided by phosphate groups. Otherwise, as occurs in sample 7, the P:Al ratio is close to 1, and the pore sizes are similar. Hence, the micelle charge density will essentially be the same in both compounds, and 68% negative sites is required. Given that sample 1 only includes ca. 47% Al_{octa}, the remaining negative charge (ca. 21%) should be provided by phosphate groups, which is in good agreement with the analytical-based estimation.

From the above, it seems evident that in the mixed aluminum phosphate/phosphonate/diphosphonate materials both charge-compensating mechanisms should be operative. Thus, in these materials, the micelle metrics is the same as for the limit homoanionic compounds. The mean density charge can be considered constant at 68% of the sites, and then the relative amount of protonated phosphate groups will grow fast with organophosphorus moiety incorporation (i.e., in the series 1−5−6 the protonated phosphates will be, at least, 22%−41%−68%, respectively).

In any case, it must be stressed that the effectiveness (and relative prevalence) of two different mechanisms (supported by the aluminum and phosphate sublattices) compensating the micelle charge is unambiguously derived from the experimental results. Although the sublattice relative charge distribution has been estimated under the hypothesis of the constancy of the micelle charge with the composition, this rough model seems reasonable because the dispersion of the pore size values is only about 8%.

A Structural Approach. To formulate a reasonable final proposal concerning the structural arrangement

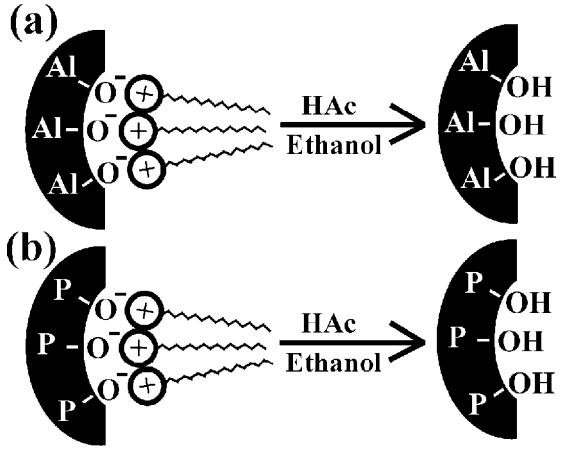

Figure 17. Schematic formation mechanism of UVM-9 materials: (a) charge compensation mechanism based on the Al sublattice (working for pure aluminum organophosphonates, samples 4 and 7); (b) cooperative mechanism provided by phosphate and aluminum centers (valid for pure ALPO (sample 1) and mixed phosphate/organophosphonate materials (samples 2, 3, 5, and 7).

in the UVM-9 materials, it can be stated that, without prejudice to the rich experimental information we have obtained, it is also true that the mere results from the chemical analyses corresponding to the mesoporous compounds 1, 4, and 7 already would suggest clearly the need for additional oxo and/or hydroxo anions to build up neutral networks. Actually, dealing with the anhydrous samples 1, 4, and 7, all our above considerations would finally lead to the following "stoichiometric" formulas: $(Al_{tetra})_{0.58}(Al_{octa}OH)_{0.52}(PO_4)_{0.79}(HPO_4)_{0.21}$ (sample 1), $(Al_{tetra})_{0.31}(Al_{octa})_{0.07}(Al_{octa}OH)_{0.86}(O,OH)_x(CH_3PO_3)$ $(0.45 \leq x \leq 0.9)$ (sample 4), and $(Al_{tetra})_{0.36}(Al_{octa}OH)_{0.76}(O,OH)_x(O_3PCH_2CH_2PO_3)$ $(0.3 \leq x \leq 0.6)$ (sample 7). Thus, as suggested by the analytical results, we can see that a certain extra negative charge is necessary to achieve the electroneutrality in the compounds including organophosphorus moieties (0.8 and 0.6 for samples 4 and 7, respectively), charge that should be provided by water-proceeding anions.

Once the stoichiometric requirements are assumed, we might conclude that the wall core of sample 1 is built up mainly from 3D alternating Al_{tetra} and phosphate groups. Very likely, the charge-supporting hydroxylated species (aluminum in octahedral coordination and hydrogenphosphate) would be located on the surface. The structure of the wall surface in sample 4 may be thought as mainly defined by an alternating network of hydroxylated octahedral aluminum and monophosphonate groups, which would be supported on a core rich in aluminum polycations. Finally, sample 7 would also contain aluminum polycations, but in contrast to sample 4, these polycations would be organized throughout the walls (from the core to the surface) by means of diphosphonate anions.

Concluding Remarks

In conclusion, periodic mesoporous aluminum phosphonates and diphosphonates (100% organophosphorus groups) have been synthesized for the first time through a generalized surfactant-assisted procedure. Together with the use of aluminum atrane complexes as an

aluminum source, the soft extraction procedure used to open the pores can be considered as the key factor to avoid the degradation of the organophosphorus groups. Moreover, the formation mechanism of the as-synthesized UVM-9 solids has been clarified by using NMR data (Figure 17). Our generalized method is applicable to the preparation of materials including other cations (different from Al) and/or phosphonic acids,[73] which implies, in turn, new opportunities for applications of mesoporous phosphates. Control of the pore size and properties, such as hydrophobicity, as well as the easy incorporation of variable amounts of organic functional groups, confer this new family of hybrid porous materials potential interest in areas such as chemical sensors, separations, catalysis, and environmental sciences.

(73) El Haskouri, J.; Guillem, C.; Latorre, J.; Beltrán, A.; Beltrán, D.; Amorós, P. Unpublished results.

Acknowledgment. This research was supported by the Spanish Ministerio de Ciencia y Tecnología (under Grants MAT2002-04239-C03-02 and MAT2003-08568-C03-01) and the Generalitat Valenciana (under Grant GRUPOS03/099). J.E.H. thanks the Ministerio de Educación, Cultura y Deporte for a postdoctoral grant.

CM048988+